

Integration Test of the High Voltage Hall Accelerator System Components

IEPC-2013-445

*Presented at the 33rd International Electric Propulsion Conference,
The George Washington University • Washington, D.C. • USA
October 6 – 10, 2013*

Hani Kamhawi^{*}, Thomas Haag[†], and Wensheng Huang[‡]. Luis Pinero[§], Todd Peterson^{**}
NASA Glenn Research Center, Cleveland, Ohio, 44135

and

John Dankanich^{††}
Marshall Space Flight Center, Huntsville, Alabama, 35801

NASA Glenn Research Center is developing a 4 kW-class Hall propulsion system for implementation in NASA science missions. NASA science mission performance analysis was completed using the latest high voltage Hall accelerator (HiVHAc) and Aerojet-Rocketdyne's state-of-the-art BPT-4000 Hall thruster performance curves. Mission analysis results indicated that the HiVHAc thruster out performs the BPT-4000 thruster for all but one of the missions studied. Tests of the HiVHAc system major components were performed. Performance evaluation of the HiVHAc thruster at NASA Glenn's vacuum facility 5 indicated that thruster performance was lower than performance levels attained during tests in vacuum facility 12 due to the lower background pressures attained during vacuum facility 5 tests when compared to vacuum facility 12. Voltage-Current characterization of the HiVHAc thruster in vacuum facility 5 showed that the HiVHAc thruster can operate stably for a wide range of anode flow rates for discharge voltages between 250 and 600 V. A Colorado Power Electronics enhanced brassboard power processing unit was tested in vacuum for 1,500 hours and the unit demonstrated discharge module efficiency of 96.3% at 3.9 kW and 650 V. Stand-alone open and closed loop tests of a VACCO TRL 6 xenon flow control module were also performed. An integrated test of the HiVHAc thruster, brassboard power processing unit, and xenon flow control module was performed and confirmed that integrated operation of the HiVHAc system major components. Future plans include continuing the maturation of the HiVHAc system major components and the performance of a single-string integration test.

I. Introduction

Electric propulsion (EP) systems performance can significantly reduce launch vehicle requirements, costs, and spacecraft mass because of its high specific impulse capability when compared to chemical propulsion. Electric

^{*} Research Engineer, Propulsion and Propellants Branch, hani.kamhawi-1@nasa.gov.

[†] Propulsion Engineer, Space Propulsion Branch, thomas.w.haag@nasa.gov.

[‡] Research Engineer, Propulsion and Propellants Branch, wensheng.huang@nasa.gov.

[§] Research Engineer, Propulsion and Propellants Branch, luis.pinero@nasa.gov.

^{**} Project Manager, Space Science Project, todd.peterson@nasa.gov.

^{††} Project Manager, Technology Development and Transfer Office, john.dankanich@nasa.gov.

propulsion systems enhance NASA's ability to perform scientific space exploration and can enable new science missions. NASA science missions to small bodies include fly-by, rendezvous, and sample return from a diverse set of targets. For example, NASA has successfully employed EP systems in the Deep Space 1 (DS1) and Dawn missions.^{1,2,3} To augment its capability to perform these and other solar system exploration missions, NASA continues to develop advanced EP technologies.⁴ Recent small body mission studies indicate that the majority of these small body missions are enabled by the use of EP, and nearly all of the small body missions of interest are enhanced with EP.⁵

NASA Science Mission Directorate (SMD) In-Space Propulsion Technology (ISPT) Project funds new EP system development for future NASA science missions.⁶ The two primary EP elements of this project are the development of NASA's Evolutionary Xenon Thruster (NEXT) ion thruster propulsion system⁷ for NASA Discovery, New Frontiers and Flagship-class missions and the development of a long-life High Voltage Hall Accelerator (HiVHAc) as a lower cost EP option for NASA Discovery-class science missions.

In addition to the mission performance benefits that can be realized with EP systems, significant cost savings can be achieved by use of Hall system when compared to gridded ion and chemical propulsion systems.⁸ A recent study by Dankanich found that a Hall thruster system can become cost competitive with alternative chemical propulsion systems if the Hall and chemical thrusters are held to the same fault tolerance.⁸ The Hall thruster system option will not only enable a wide range of Discovery-class missions, but will enable science return far greater than the chemical alternatives. Table 1 presents the cost savings that a Hall thruster propulsion system will provide over a gridded-ion propulsion system.

Table 1. Comparison of chemical and electric propulsion system (NEXT ion and Hall) delta costs for NASA Discovery class missions.

Thruster	Configuration	Cost Δ\$M
Chemical Bipropellant	1+0	Baseline
NEXT 1 st User	1+1	+26.5
NEXT n th User	1+1	+7.0
Hall 1 st User	1+1	+6.5
Hall n th User	1+1	+0.5

This paper is organized as follows: Section 2 presents recent mission analysis results that highlight the mission performance benefits that a HiVHAc propulsion system can deliver over SOA BPT-4000. Section 3 provides an overview of the HiVHAc system that is currently being developed by NASA Glenn. Section 4 presents component characteristic tests, including: results from performance and voltage-current (V-I) characterization of the HiVHAc thruster in vacuum facility 5 (VF5), results from testing of the enhanced brassboard power processing unit, and results from flow tests of the VACCO xenon flow control module. Section 5 presents results from the integrated tests of the HiVHAc system components and lists projected HiVHAc system performance. Finally, section 6 summarizes the paper content.

II. Mission Analysis

In 2004, mission studies found that for certain NASA Discovery-class science missions, a 4 kW-class Hall thruster system resulted in substantial cost and performance benefits when compared to the NASA Solar Electric Propulsion Technology Application Readiness (NSTAR) and NEXT ion engine.^{9,10,11,12}

Recently, additional mission studies were performed to evaluate the performance of the HiVHAc 3.9 kW thruster and a SOA 4.5 kW Aerojet-Rocketdyne flight Hall thruster designated BPT-4000.¹³ The mission studies results were updated with recent HiVHAc and BPT-4000 throttle tables that reflect improved and extended thruster operating performance results.^{14,15} The recent mission studies utilized the HiVHAc performance results from testing in vacuum facility 12 (VF12) which included thruster operation in two modes: a high-specific impulse and a high thrust-to-power mode.

Additionally, the BPT-4000 throttle table used in these mission studies incorporated results from recent BPT-4000 tests at high discharge voltage that demonstrated BPT-4000 thruster operation at high specific impulse.¹⁵ These mission studies included evaluation of the HiVHAc and BPT-4000 thruster operation for four NASA Discovery-

class design reference missions (DRMs), two New Frontiers-class DRMs, and one Flagship-class DRM. The evaluated missions included:

- Discovery-class Vesta-Ceres rendezvous mission (i.e., Dawn Mission), which has both time constraints and a very high post launch ΔV , requiring both moderate thrust-to-power and a higher specific impulse than a conventional Hall thruster;
- Discovery-class Koppf comet rendezvous (CR) mission, which has few constraints and does not thrust in gravity wells (this favors a high specific impulse throttle table);
- Discovery-class Near-Earth Asteroid Return Earth Return (NEARER) mission;
- Discovery-class Nereus sample return (NSR) mission which is a relatively low- ΔV mission with time constraints, favorable for a higher thrust-to-power thruster;
- New Frontiers-class Wirtanen comet surface sample return (CSSR), a 2004 New Frontiers Design Reference Mission target with a 12 km/s post launch ΔV for a 7 year sample return;
- New Frontiers-class Churyumov-Gerasimenko (C-G) CCSR, a 2012 Decadal Survey design reference mission target with a 7-10 km/s post launch ΔV for a 12 year sample return, depended on the thruster;
- Flagship-class Uranus Orbiter with probe mission from the 2012 Planetary Science Decadal Survey design reference mission. The electric propulsion is used to augment the mass to Uranus to allow for a chemical orbit insertion and satellite tour.

Results from the mission studies indicated that the HiVHAc thruster was able to exceed the needs of all the evaluated missions except for the Uranus Orbiter Flagship-class mission. For the various Discovery- and New Frontiers-class missions that were evaluated, the HiVHAc thruster performance was sufficient; moreover, the high thrust-to-power throttle table operation typically provided higher performance than the high specific impulse thruster operation. The BPT-4000 SOA thruster with its extended power and discharge voltage throttle table had sufficient performance for the Koppf CR, NEARER, and Nereus SR missions but had insufficient performance for the Dawn mission. In addition, the BPT-4000 thruster had insufficient performance for the two New Frontiers-class and one Flagship-class missions that were evaluated. A summary of the results from the various mission performance studies is presented in Figs. 1-4.

Figure 1 presents the mission performance results for the Discovery-class Dawn and Kopf CR missions, Fig. 2 presents the results for the Discovery-class NEARER and NSR missions, Fig. 3 presents the results for the New Frontiers-class Wiraten CCSR and C-G CCS missions, and Fig. 4 presents the Flagship-class Uranus Orbiter with probe mission.

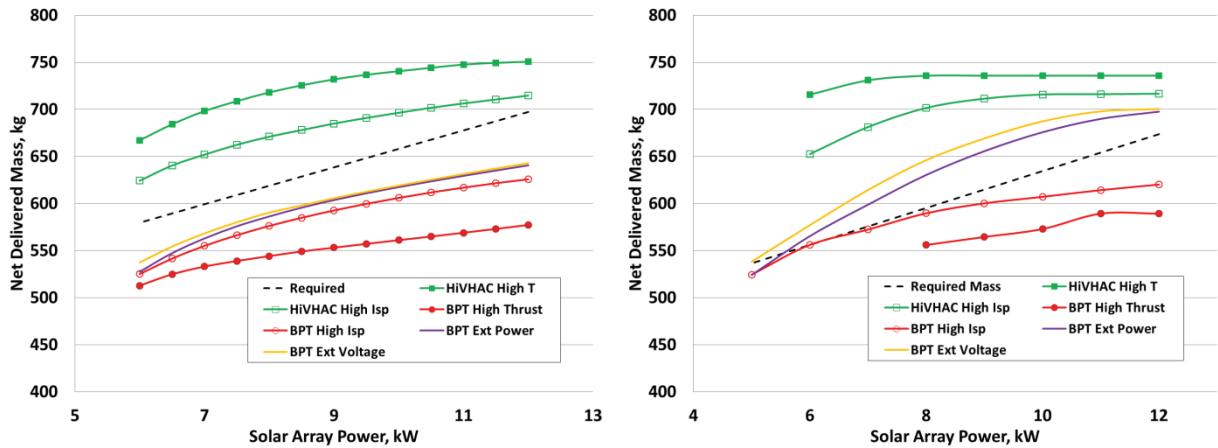


Figure 1. HiVHAc and BPT-4000 mission performance for the Dawn (left) and Kopf CR (right) Discovery-class missions.

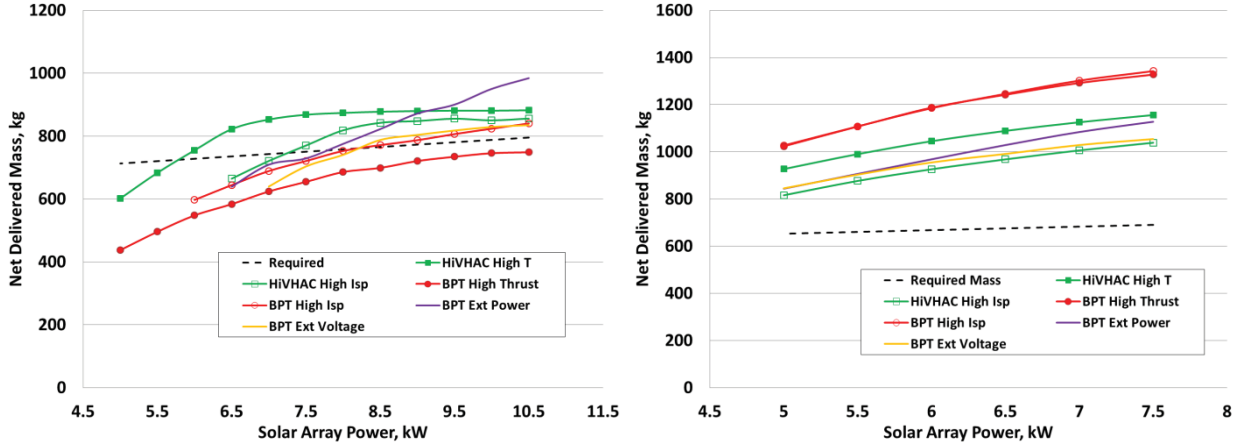


Figure 2. HiVHAc and BPT-4000 performance for the NEARER (left) and NSR (right) Discovery-class missions.

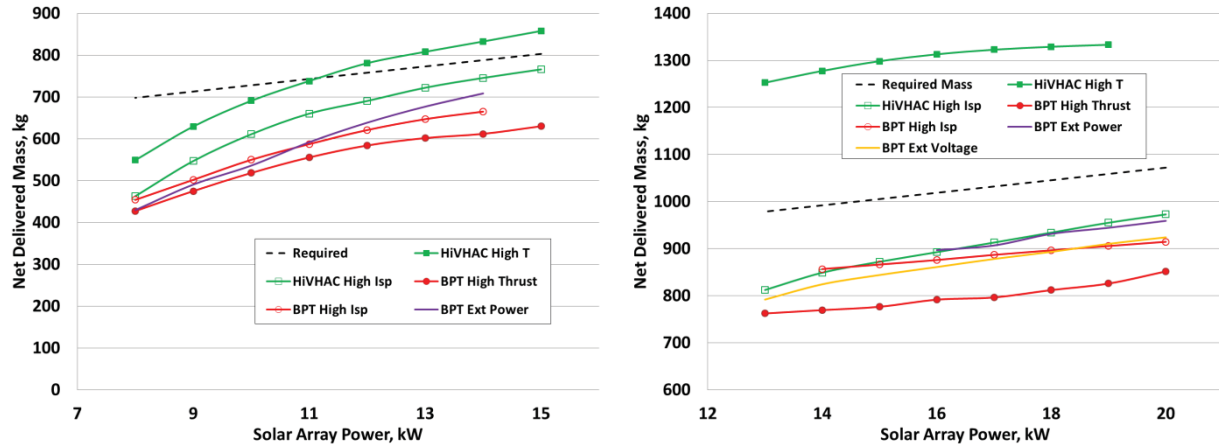


Figure 3. HiVHAc and BPT-4000 performance for the Wiraten CSSR (left) and C-G CSSR (right) New Frontiers-class missions.

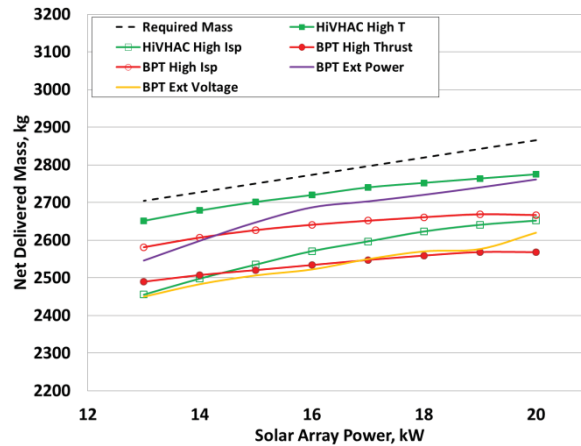


Figure 4. HiVHAc and BPT-4000 performance for the Uranus probe Flagship mission.

III. High Voltage Hall Accelerator Propulsion System

The major elements of the high-specific impulse long-life Hall propulsion system that are being developed and matured include the HiVHAc engineering development unit (EDU) thruster, power processing unit (PPU), and xenon feed system (XFS) as is shown in Fig. 5. The EDU 2 thruster, thereafter referred to as EDU, development and testing are being performed by NASA Glenn and Aerojet-Rocketdyne. The EDU thruster has undergone functional, performance, and qual-level random vibration tests.¹⁴ For the PPU development, the HiVHAc project has been leveraging and evaluating PPU developments that have been sponsored by industry and NASA's Small Business Innovative Research (SBIR) program but that can apply directly to a Hall propulsion system. The most mature PPU is a brassboard (BB) unit developed by Colorado Power Electronics (CPE).¹⁶ The first generation BB unit was tested in vacuum for over 2,000 hours, and that led to the development of a BB2 unit that leveraged and incorporated the lessons learned during BB1 tests.¹⁷ For the xenon feed system (XFS) development, the HiVHAc project and Air Force Research Laboratory (AFRL) have furthered the development of an ISPT-funded advanced xenon flow control module (XFCM) by VACCO Industries.¹⁴

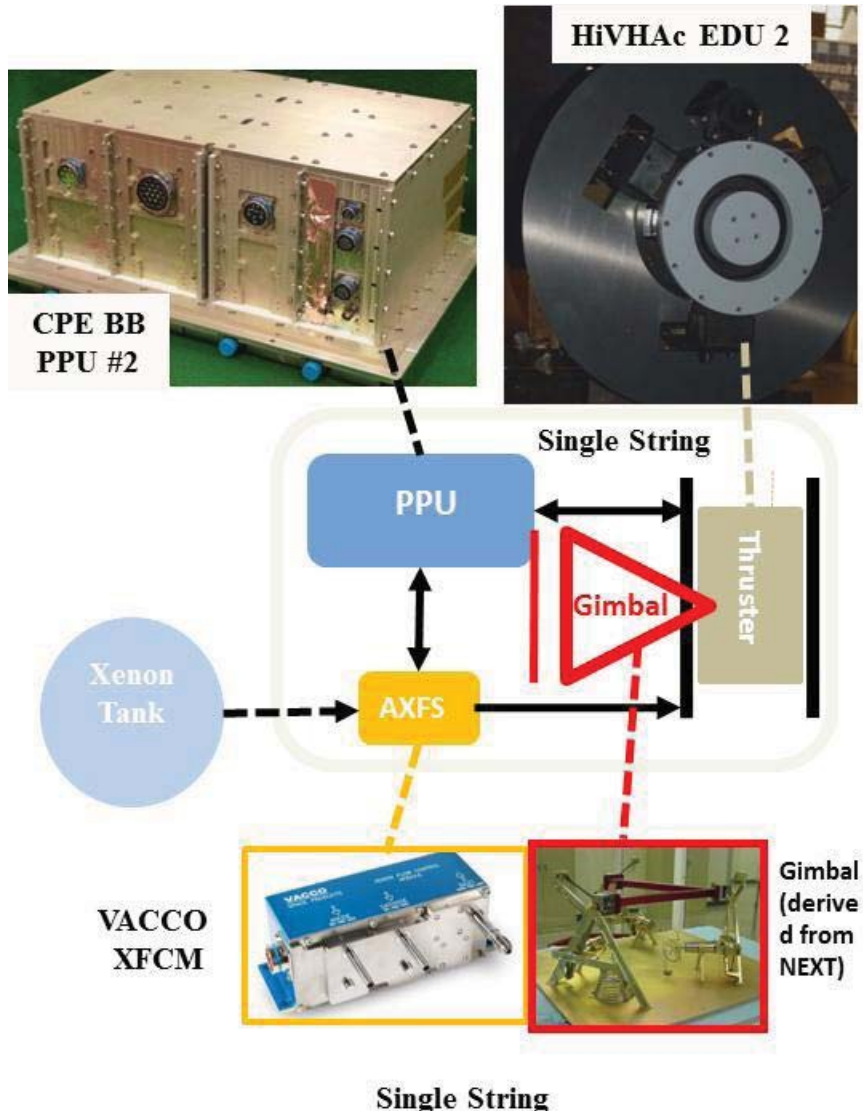


Figure 5. HiVHAc Propulsion System Single String layout.

IV. HiVHAc System Component Testing

Tests of the various HiVHAc system components were performed at NASA Glenn in a number of different vacuum facilities that will be detailed in this section. The HiVHAc system components that were evaluated include the HiVHAc EDU thruster, enhanced CPE BB PPU, and the VACCO XFCM. Section 4A presents that various facilities, test hardware, and diagnostics that were implemented during the HiVHAc system components tests and presents that results from these tests. Sections B.1 and B.2 presents the EDU thruster performance and V-I characterization test results, respectively. Section C presents the enhanced CPE BB PPU, thereafter referred to as BB2, discharge module evaluation results. Section D presents the VACCO XFCM VF5 and VF12 test results.

A. Experimental Facilities and Test Hardware

The experimental hardware utilized the HiVHAc SSIT includes VF5, a four mass flow control laboratory propellant feed system, high voltage power supply, an inverted pendulum thruster stand, and data acquisition system.

A.1 Vacuum Facility 5, 12, and 70

Testing of the HiVHAc EDU thruster was performed in VF5 at NASA Glenn. Vacuum facility 5 main chamber is 4.6 m in diameter and is 18.3 m long. VF5's main port (designated E55) is 1.8 m in diameter and is 2.5 m long. VF5 can be evacuated with cryopanels and oil diffusion pumps. For this test campaign the HiVHAc thruster was placed in VF5's main volume at the facility midsection by the facility cryopanels. That was done to assure that the lowest possible background pressure conditions were attained during thruster operation. Figure 6 shows a picture of the HiVHAc thruster mounted inside VF5. Facility pressures were monitored with four ion gauges, three of which were mounted next to the thrust stand, fourth being on the facility wall. Manufacturer specifications state that the ion gauges are accurate to $\pm 6\%$ of reading. The positions of the gauges are shown in Fig. 7. Ion gauges 1 and 2 are both facing downstream while ion gauge 3 is facing upstream. Ion gauge 1 and 2 agree to within 10% of each other. Ion gauge 3 reports 0.63 to 0.72 times the reading as ion gauge 2. Ion gauge 2 readings were used to determine the number of multiples of the lowest achievable background pressure that the thruster was experiencing. Vacuum facilities 12 and 70 description has been presented in previous publications and will not be detailed here.¹⁴

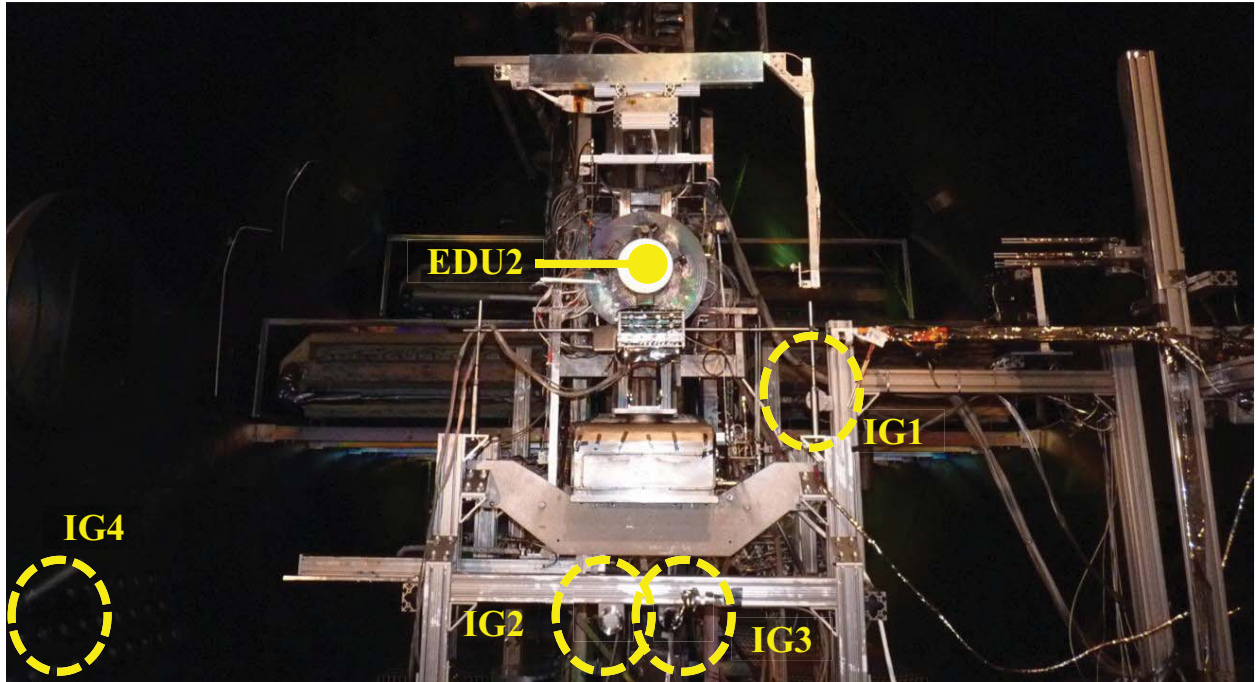


Figure 6. The HiVHAc EDU thruster mounted on the inverted pendulum thruster stand inside VF5, denoted on the photograph are the locations of the four ion gauges that were used to monitor the pressure in the vicinity of the thruster.

A.2 Laboratory Propellant Feed System

A laboratory propellant feed system was used in the HiVHAc component tests. The propellant feed system utilized four mass flow controllers (MFCs). A 200 sccm MFC was used to supply xenon to the XFCM unit. A 100 sccm MFC supplied xenon to the thruster propellant manifold (i.e, anode). For cathode 1, a 10 sccm MFC unit was used. Finally, for the cathode 2 and cathode 1 auxiliary flow a 50 sccm MFC was used.¹⁸ All MFC units were calibrated prior and after with xenon. The laboratory feedsystem is shown in Fig. 7 and a closeup of the VACCO XFCM setup in VF5 is shown in Fig. 7. The MFC calibration curves indicated that the anode and cathode flow rates uncertainty is $\leq 1\%$ of set value.

A.3 Power Console

For this test campaign the thruster was mostly powered with the BB1, shown in Fig. 6. The BB1 was placed outside the vacuum chamber to allow for use of a laboratory power supply during thruster V-I characterization tests. The BB1 PPU has demonstrated over 2,000 hours of operation in vacuum as was reported earlier.¹⁹ The PPU is powered with a 0-160 Vdc 90 A power supply. The operation of the BB1 is controlled with a control console built by CPE. The high-voltage laboratory power supply that was used during the V-I tests is a 15 kW 600 V capable power supply that was borrowed from The Aerospace Corp.

A.4 Inverted Pendulum Thrust Stand

A Null-type water-cooled inverted pendulum thrust stand was implemented during thruster performance evaluation. The power cables were fed from the vacuum feed thru to the thruster using a “water fall” configuration to minimize the thermal drift of the thrust stand readings. In-situ thrust stand calibrations were performed prior, during, and after thruster testing. In addition, during thruster testing the thruster was periodically turned off to measure the thrust stand thermal drift magnitude, and the corrections were incorporated in the reported thrust. Thrust measurement uncertainty was estimated at 2% of measured value.

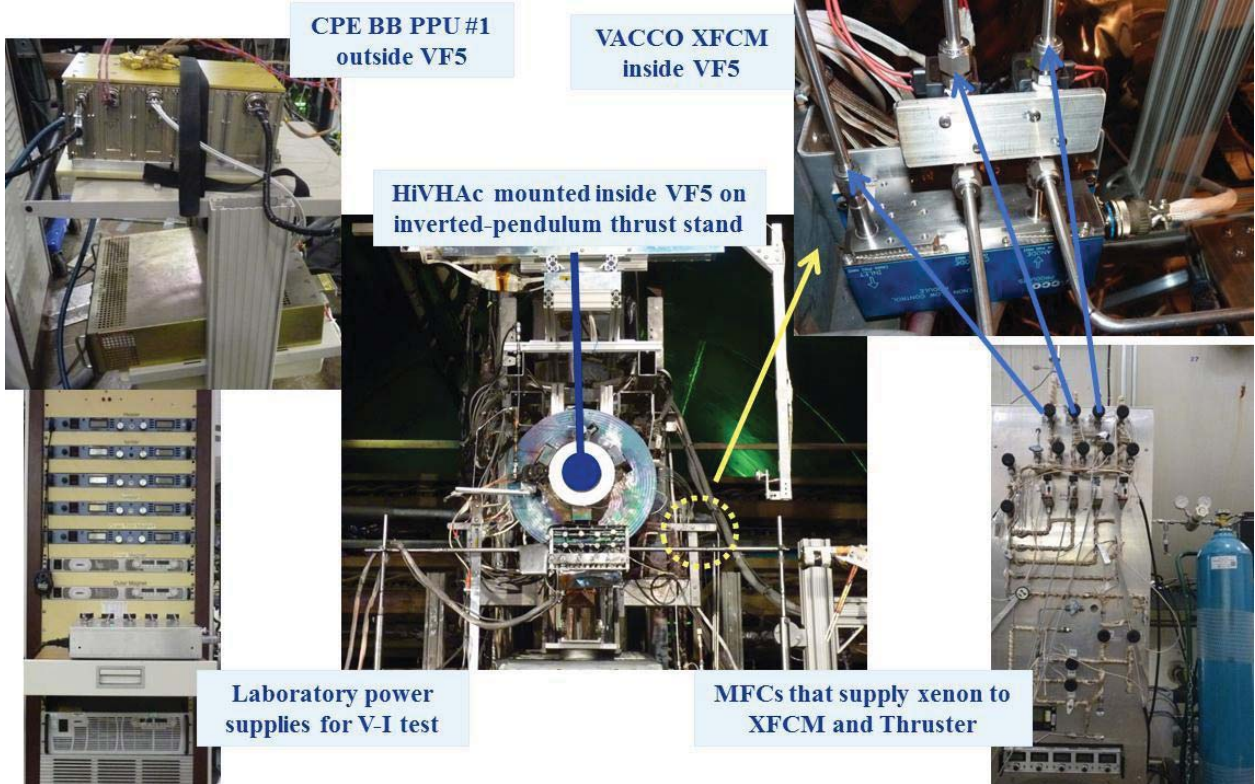


Figure 7. HiVHAc System Components test hardware.

A.5 Data Acquisition

A data logger was used to measure and record the thruster operating parameters. The data logger measurements were calibrated using a calibrated meter. The data logger recorded the various thruster operating currents, operating voltages, thruster component temperatures, and facility pressure in the vicinity of the thruster as was shown in Fig. 6.

A.6 Diagnostics

A number of diagnostics were implemented during this test campaign. This extensive set of diagnostics was used to take full advantage of the opportunity to test HiVHAc EDU in VF5. These diagnostics included:

- Plasma diagnostics: The diagnostics suite a near-field Faraday probe that mounted on axial and rotary stages, far-field retarding potential analyzer (RPA), E×B, and Langmuir probe. Results from the Faraday, RPA, E×B, and Langmuir probes are reported by Huang *et al.*, in a companion paper.²⁰ In addition to the above diagnostics, an Air Force Research Laboratory (AFRL) high speed Langmuir probe (HSLP) rake was implemented in this test. Analysis of the HSLP data is on-going and will be published at a later time;
- Fast camera imaging of the HiVHAc thruster discharge was performed using a FAST camera. Analysis of the FAST CAM images is on-going and will be presented at a later time;
- Type-K thermocouples were used to monitor the temperature of various thruster components during this test campaign. Analysis of the results is on-going and will be presented at a later time; and
- Infrared camera imaging of the HiVHAc thruster using a FLIR Aerospace camera that was placed inside a pressurized enclosure inside VF5 4 m away from the thruster. Results from the thermocouple and IR camera measurements will also be presented a later time.

Figure 8 shows a picture of the various diagnostics used during this test campaign.

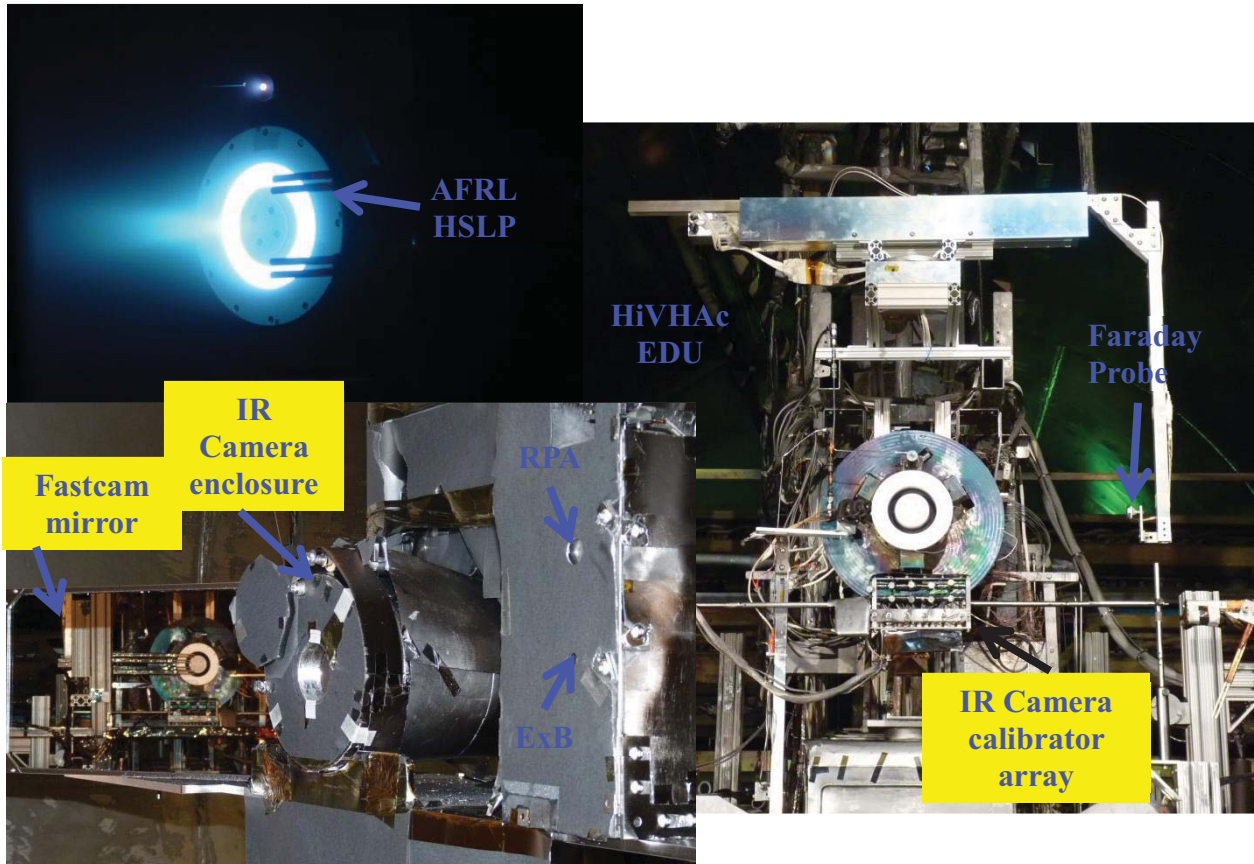


Figure 8. Photograph showing the various diagnostics implemented during the HiVHAc thruster test campaign at NASA Glenn's VF5.

B. HiVHAc Engineering Development Unit Thruster Characterization Tests

B.1 Test Objectives

The main objectives of HiVHAc EDU thruster tests in VF5 were:

1. Characterize the performance of the HiVHAc thruster under the lowest attainable background pressure conditions in VF5;
2. Obtain the V-I profiles of the HiVHAc thruster to characterize thruster stability under various thruster flow rates and electromagnet current settings; and
3. Evaluate impact of varying background pressure magnitude on thruster performance and operating characteristics.

Secondary test objectives included performing thermal characterization tests by measuring thruster components temperatures with thermocouples and the FLIR IR camera, evaluate effect of varying cathode flow split and position on thruster operation, evaluate effect of auxiliary flow in the vicinity of the cathode on thruster performance, and measurement of near and far-field plasma properties to assess thruster loss mechanisms.

In this paper the results from main objectives 1 and 2 will be presented and discussed. A companion paper will present and discuss the results from the background pressure sensitivity study.²¹ Another companion paper will discuss results from near and far-field plasma measurements that were taken during the background pressure sensitivity investigation.²⁰ Results from the thermal characterization tests, and FAST camera measurements will not be discussed in this paper but will be presented in a later publication.

B.2 HiVHAc EDU Thruster Performance Evaluation

The HiVHAc EDU thruster performance was characterized for the entire throttle range of the thruster in VF5. The thruster performance was evaluated for discharge voltages between 200 and 650 V. Table 2 below lists the thruster operating condition where the thruster performance was characterized. For the thruster performance characterization, BB1 and laboratory XFS were used. Although the performance acceptance test (PAT) of the HiVHAc thruster was performed in April/May of 2012 at NASA Glenn's VF12, the tests performed in VF5 were performed at background pressure levels that are approximately 6-7 times lower than during the PAT in VF12.¹⁴ Investigation of the effects of background pressure on thruster performance will be reported in two companion papers.^{20,21}

Table 2. HiVHAc EDU2 thruster performance characterization test throttle operating conditions.

V _d , V	Discharge Power, W								
	300	500	1000	1,500	2,000	2,500	3,000	3,500	3,900
200	•	•	•	•					
300	•	•	•	•	•				
400		•	•	•	•	•	•		
500		•	•	•	•	•	•	•	•
600		•	•	•	•	•	•	•	•
650		•	•	•	•	•	•	•	•

For this test campaign, VF5 was equipped with four ion gauges that were positioned in close proximity to the thruster which were shown previously in Fig. 7.

The discharge specific impulse and thrust efficiency of the thruster were calculated using

$$(I_{sp})_d = \frac{T}{\dot{m}_a g} \quad \text{and} \quad (\eta_t)_d = \frac{T^2}{2\dot{m}_a P_d} \quad (1) \text{ and } (2)$$

Total specific impulse and efficiency were calculated using

$$I_{sp} = \frac{T}{(\dot{m}_a + \dot{m}_c)g} \quad \text{and} \quad \eta_t = \frac{T^2}{2(\dot{m}_a + \dot{m}_c)P_{Total}} \quad (3) \text{ and } (4)$$

where P_{Total} includes the discharge, electromagnet, and cathode keeper power. For the total performance results that will be reported herein, the electromagnet power used in the calculation is based on thruster electromagnet voltage when it is at steady state temperature. This assures that we are accounting for the highest attainable magnet power in the thruster's total efficiency calculation.

For the EDU thruster, Fig. 9 presents the discharge specific impulse and discharge efficiency profiles, whereas, Fig. 10 presents the total specific impulse and thrust efficiency profiles. Results of VF5 tests indicate performance levels that are lower than levels demonstrated during the performance acceptance test (PAT) of EDU in VF12.¹⁴ The performance evaluation in VF5 indicates that the thruster performance was lower than in VF12 for all power level and discharge voltage operating conditions. For example, at a discharge voltage of 400 V and power level of 3 kW, VF5 tests indicated a discharge specific impulse of 2,119 sec and a discharge efficiency of 55%, whereas, VF12 tests indicated a discharge specific impulse of 2,106 sec and a discharge efficiency of 56.5%. For thruster operation at 3.9 kW and 500 V, VF5 tests indicate a discharge specific impulse of 2,407 sec and a discharge efficiency of 55%; whereas, VF12 tests indicate a discharge specific impulse of 2,490 sec and a discharge efficiency of 58%. For thruster operation at 3.9 kW and 600 V, VF5 tests indicate a discharge specific impulse of 2,580 sec and a discharge efficiency of 53%; whereas, VF12 tests indicate a discharge specific impulse of 2,790 sec and a discharge efficiency of 63.5%. Reference 21 presents the results for the facility background pressure sensitivity study.

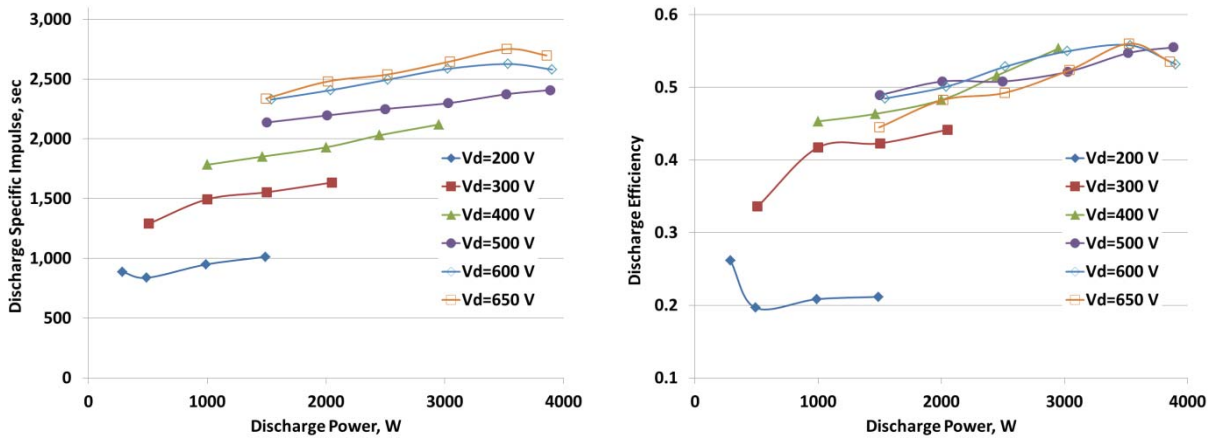


Figure 9. Discharge specific impulse profiles for the HiVHAc EDU thruster for discharge voltages between 200 and 650 V during tests at NASA Glenn's VF5.

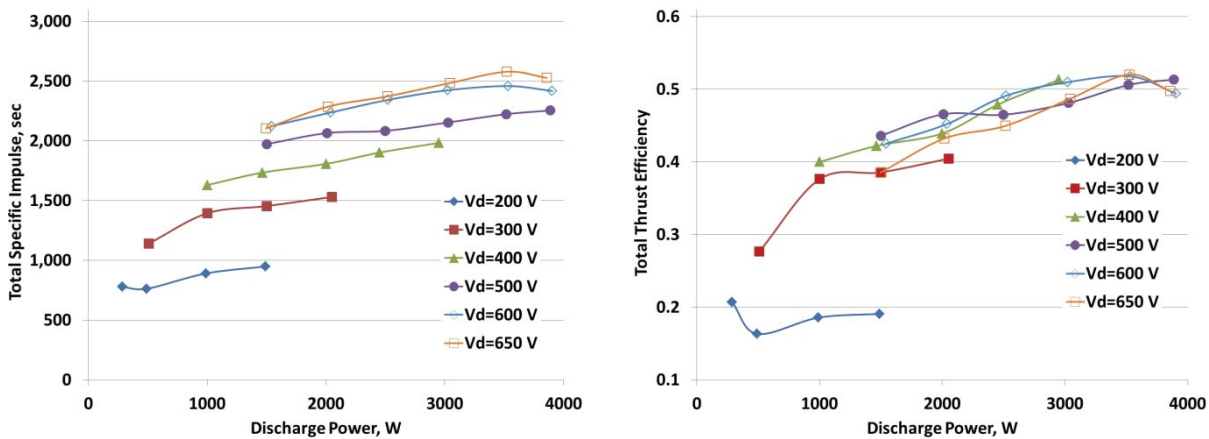


Figure 10. Total specific impulse profiles for the HiVHAc EDU thruster for discharge voltages between 200 and 650 V during tests at NASA Glenn's VF5.

B.3 HiVHAc EDU Thruster Voltage-Current Characterization

The voltage-current (V-I) profiles of the HiVHAc EDU2 thruster were obtained for various thruster flow rates and electromagnet settings. These characteristics were performed to assess the stability of the thruster operation under various operating settings and to guide the selection of optimized thruster operating settings. Additionally, from the HiVHAc thruster perspective, to stably operate the thruster with the lowest electromagnet current magnitude (with margin). This reduces the electromagnets internal temperatures and alleviates any potential thermal issues that may degrade the thruster electromagnets integrity.

The EDU thruster V-I profiles were acquired for anode flow rates of 2, 3, 4, 5, 6, 6.5, and 7 mg/s for electromagnet currents that ranged from a nominal value of I_0 to 100% above that value ($2 \cdot I_0$). For all test conditions, the thruster discharge voltage was varied between 200 and 600 V at 1 V increments with a voltage ramp rate of 1V/s. Additional V-I profiles were performed at elevated background pressure conditions, those results will be reported and discussed in a companion publication.¹⁸ The V-I characterization tests used a 15 kW 600 V power supply that was borrowed from The Aerospace Corp. A program by The Aerospace Corp. was used to perform and record the V-I profiles of the thruster.

The thruster V-I profiles provide insights into thruster behavior and stability under different electromagnet settings. The V-I profiles presented in Figs 14 through 20 have four distinct regions and trends that provide insights into thruster behavior and operation at the different electromagnet settings, they are:

- A negative sloped region where as the discharge voltage is increased the discharge current decreases; in this region the thruster discharge current oscillations were large;
- A flat region where as the discharge voltage is increased the discharge current, for the most part, was unchanged; this region was characterized by relatively small discharge current oscillations and is desirable;
- A positive sloped region where as the discharge voltage is increased the discharge current increases; in this region the discharge current oscillations magnitude was relatively greater than the flat region but was less than their magnitude in the negative region; and
- A hump region where the discharge current increases rapidly with the discharge voltage in a narrow voltage region, this typically resulted in large magnitude discharge current oscillations.

For the 2 mg/s case, Fig. 11, the V-I profiles indicate that the thruster is mostly operating with a positive slope. The profiles indicate that for discharge voltages between 250 and 450 V, the electromagnet current can be set to $1.25 \cdot I_0$ and $1.5 \cdot I_0$ and for discharge voltages above 450 V an electromagnet setting of $1.5 \cdot I_0$ to $2 \cdot I_0$ provided for stable operation. For the 3 mg/s case, Fig. 12, the V-I profiles indicate that the thruster is mostly operating with a positive slope except for discharge voltages between 200 and 250 V. The profiles indicate that for discharge voltages between 250 and 450 V, the electromagnet current can be set to $1.5 \cdot I_0$ and higher. For discharge voltages above 450 V an electromagnet setting of $1.75 \cdot I_0$ and $2 \cdot I_0$ resulted in stable thruster operation.

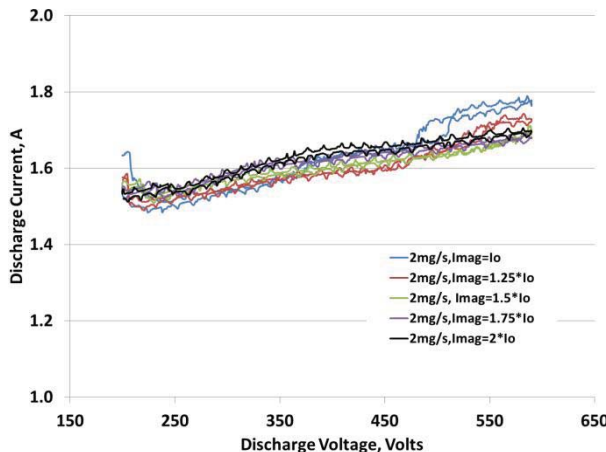


Figure 11. V-I profiles of HiVHAc EDU thruster for a flow rate of 2 mg/sec and discharge voltages between 200 and 600 V.

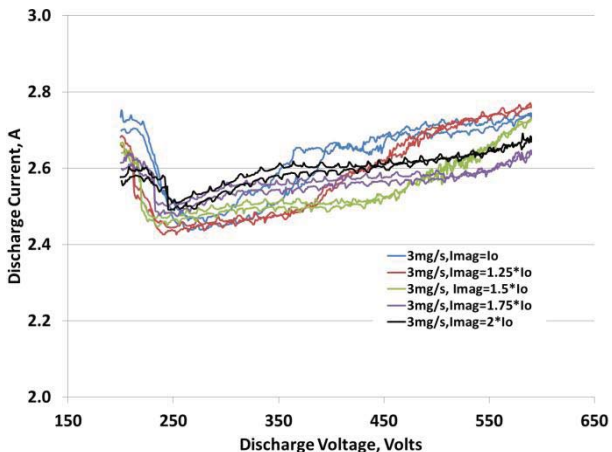


Figure 12. V-I profiles of HiVHAc EDU thruster for a flow rate of 3 mg/sec and discharge voltages between 200 and 600 V.

For the 4 mg/s case, presented in Fig. 13, the V-I profiles indicate that for electromagnet current magnitudes of I_{lo} and $1.25 \cdot I_{\text{lo}}$, the negative slope region extends from 200 to 250 V, then it is followed by a positive slope region from 250 to 300 V, then a hump region appears at a discharge voltage of approximately 300 V. For discharge voltages above 350 V the discharge current magnitude for I_{lo} and $1.25 \cdot I_{\text{lo}}$ is greater than at higher electromagnet currents. The V-I profile for $1.5 \cdot I_{\text{lo}}$ indicates that a mostly flat region exists between discharge voltages of 225 and 350 V, above 350 V the discharge current starts to increase at a rapid rate. For electromagnet currents of $1.75 \cdot I_{\text{lo}}$ and $2 \cdot I_{\text{lo}}$ and for discharge voltages above 250 V, the V-I profiles indicate a positive sloped profile. In summary, to attain stable thruster operation at an anode flow rate of 4 mg/s with a minimized discharge current, the thruster should be operated with an electromagnet current of $1.5 \cdot I_{\text{lo}}$ below 350 V and an electromagnet current of $1.75 \cdot I_{\text{lo}}$ above 350 V.

For the 5 mg/s case, presented in Fig. 14, the V-I profiles indicate that it is not desirable to operate the thruster at an electromagnet currents of I_{lo} due to the formation of a “hump” region that is followed by a negative slope region for discharge voltages between 250 and 450 V. At an electromagnet of $1.25 \cdot I_{\text{lo}}$ a negative sloped region exists between 200 and 250 V, a hump region starts forming at 300 V. At discharge voltages above 350 V a mostly flat region exists but with discharge current magnitudes that are higher than at electromagnet currents of $1.5 \cdot I_{\text{lo}}$ and above. For an electromagnet current of $1.75 \cdot I_{\text{lo}}$ and for discharge voltages between 250 and 400 V, the V-I profiles indicate a mostly flat region, a positive slope region appears at 400 V, and then transitions to a flat region above 450 V. For an electromagnet current of $2 \cdot I_{\text{lo}}$, a flat region exists between 250 and 450 V, then a positive region appears from 450 to 500 V, then the V-I profile becomes flat. From Fig. 14 and for a flow rate of 5 mg/s, the most stable and optimized thruster operation can be attained by operating with an electromagnet current of $1.25 \cdot I_{\text{lo}}$ for discharge voltages between 250 and 300 V, then transitioning to an electromagnet current of $1.75 \cdot I_{\text{lo}}$ for discharge voltages between 300 and 400 V and finally transiting to an electromagnet current of $2 \cdot I_{\text{lo}}$ for discharge voltages above 400V.

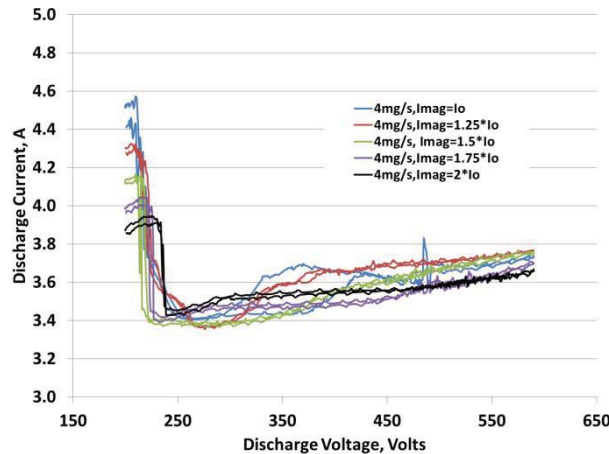


Figure 13. V-I profiles of HiVHAc EDU thruster for a flow rate of 4 mg/sec and discharge voltages between 200 and 600 V.

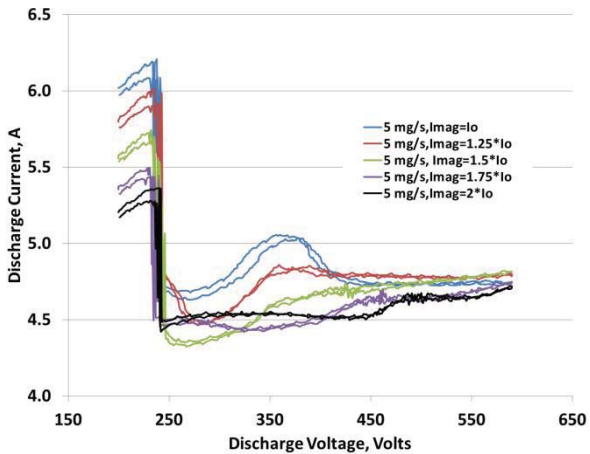


Figure 14. V-I profiles of HiVHAc EDU thruster for a flow rate of 5 mg/sec and discharge voltages between 200 and 600 V.

The V-I profiles for the anode flow rate of 6, 6.5, and 7 mg/s are presented in Figs. 15, 16, and 17, respectively. Figures 15-17 are qualitatively very similar. No stable thruster operation could be attained at an electromagnet current of I_{lo} , at I_{lo} the discharge current magnitude and oscillations were too large. As the electromagnet current was increased to $1.25 \cdot I_{\text{lo}}$ thruster performance started to improve, but at $1.25 \cdot I_{\text{lo}}$ the discharge current magnitude was still not minimized and there existed a pronounced hump region that was followed by a negative sloped region. Increasing the electromagnet current to $1.5 \cdot I_{\text{lo}}$ continued to improve thruster operation, at this electromagnet setting the lowest discharge current is obtained for discharge voltages between 250 and 300 V, however, for discharge voltages above 300 V, the discharge current magnitude was higher than was obtained at the higher electromagnet settings. For an electromagnet current of $1.75 \cdot I_{\text{lo}}$, Figs. 18-20 indicate that a narrow region of optimized operation for discharge voltages below 350 V exists but it continues to shift to the left as the anode flow rate is increased. At an electromagnet current of $2 \cdot I_{\text{lo}}$ and at discharge voltages above 350, 325, and 300 V for flow rates of 6, 6.5, and 7 mg/s, respectively, minimized discharge thruster operation is obtained.

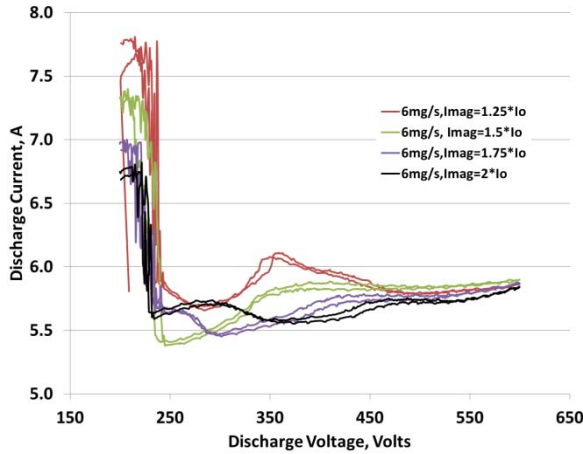


Figure 15. V-I profiles of HiVHAc EDU thruster for a flow rate of 2 mg/sec and discharge voltages between 200 and 600 V.

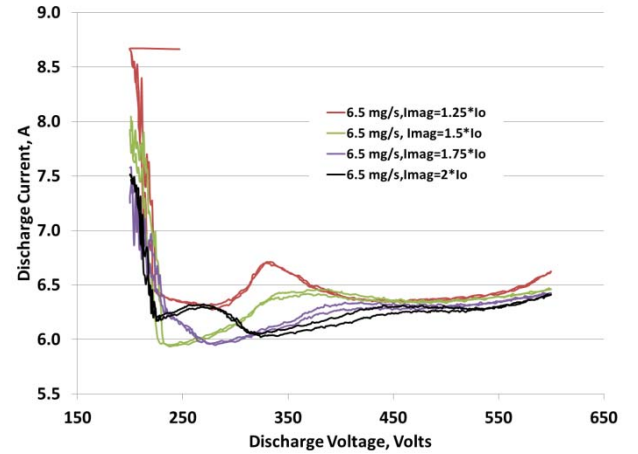


Figure 16. V-I profiles of HiVHAc EDU thruster for a flow rate of 2 mg/sec and discharge voltages between 200 and 600 V.

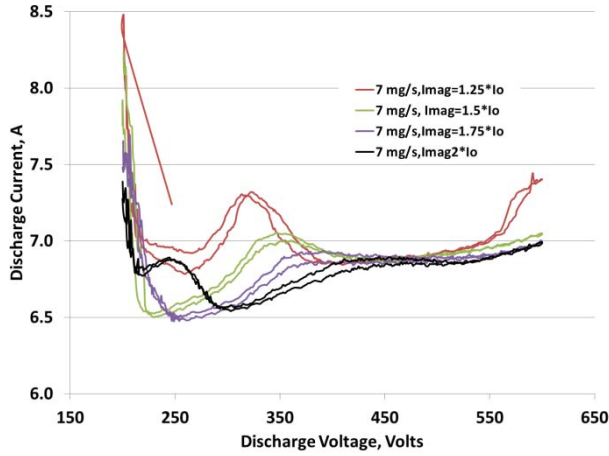


Figure 17. V-I profiles of HiVHAc EDU thruster for a flow rate of 2 mg/sec and discharge voltages between 200 and 600 V.

Finally, this set of V-I profiles provides insights into the HiVHAc thruster regions of stability. The profiles presented in Figs. 11-17 indicate that, at the various anode flow rates, “wide” regions of stable thruster operation at electromagnet current settings that are within the operational limits of the thruster exist. Further analysis of the presented V-I profiles will be performed in conjunction with the thruster performance and thermal data that were collected in this test. Additional profiles will also be performed where high frequency monitoring of the discharge voltage and current oscillations will be conducted to further assess thruster stability.

C. Colorado Power Electronics Enhanced Brassboard Power Processing Unit Characterization Test

C.1 Test Objectives

NASA Glenn is pursuing the development of a PPU with CPE through the Small Business Innovative Research (SBIR) program. Under a previous Phase 2 effort, CPE developed a brassboard PPU, designated BB1, which was delivered to NASA Glenn in 2010. The BB1 includes two 2 kW discharge modules that operate in parallel to generate up to 725 V from an input voltage range of 80 to 160 V. It also has two electromagnet supplies and cathode heater and keeper supplies with a high voltage ignition circuit. The BB1 was tested for more than 2,000 hours in vacuum conditions, with resistive load and the HiVHAc thruster, and at room and elevated base plate temperatures. Performance and thermal test data were shared with CPE to support the development of an enhanced brassboard PPU, designated BB2, that was delivered to Glenn in May 2013. Some of the design enhancements include:

- Flight-like thermal and structural designs;
- Provisions for a printed circuit board to control and communicate with the VACCO XFCM;
- EEE circuit components that have radiation hardened space qualified equivalence; and
- Improved manufacturability.

The objectives of the BB2 test is to evaluate the unit's operation in vacuum for the unit's full range of input voltages, output voltages, and power levels.

C.2 BB2 Discharge Modules Performance

The BB2 was initially subjected to functional testing at atmospheric conditions. After that it was installed in vacuum facility 70 (VF70) and baked-out in preparation for vacuum testing. The BB2 PPU was then performance tested in vacuum up to full power conditions.

The efficiency of the discharge supply in the BB2 was measured during vacuum operation. The input voltage was varied from 80 to 160 V in 20 V increments and the discharge voltage from 300 to 600 V in 100 V increments and at a maximum voltage of 650 V. Sense leads measured the voltage at the PPU input to eliminate voltage drops in the input cables. Limitations with the resistive load precluded operating the PPU at high output voltage and low power conditions.

To date, BB2 has been subjected to a 1,500 hours burn-in test at full power (at an input voltage of 80 V, output voltage of 650 V at a discharge power of 3.9 kW). Figures 18-22 present the discharge modules efficiency profiles for output voltages of 300, 400, 500, 600, and 650 V as a function of discharge (output) power. In general, results in Figs. 18-22 indicate that the discharge module efficiency increases as the discharge module output power is increased, and that efficiency decreases as the input voltage is increased. Results in Figs. 21 and 22 indicate that at an input voltage of 80 V, peak module efficiency of 96.3% is attained for discharge voltages of 600 and 650 V at 3.9 kW. Figures 19 and 20 show that at a discharge voltage of 400 and 500 V the discharge module efficiency is 95.5% and 95.7%, respectively, at 3.9 kW. For a discharge voltage of 300 V, discharge module efficiency was evaluated at a peak power of 3 kW because we wanted to limit the discharge current to 10 A, the results indicate that discharge modules had an efficiency of 95% at 300 V and 3 kW as is shown in Fig. 18. Figure 18-22 indicate that as the input voltage is increased from 80 to 160 V, the discharge module efficiency decreases. For example, for an output voltage of 600 and 650 V, as the input voltage is increased from 80 to 120 then to 160 V, the discharge module efficiency decreases from 96.3% to 95.5% to 94.6%, respectively. Throughout the entire range of operating conditions, the discharge modules output currents were within 2.7% of each other, which suggest they share the output very well.

Breadboard 2 total efficiency was measured during operation at 3.9 kW output power at 650 V for an input voltage of 80 V. During the test, the inner and outer electromagnet currents were set to their anticipated peak operational magnitudes. Test results indicated that the PPU measured efficiency was 96% (compared to 96.3 discharge module efficiency).

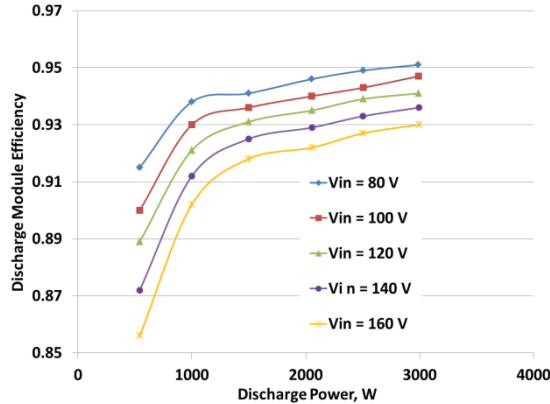


Figure 18. Discharge module efficiency for an output voltage of 300 V.

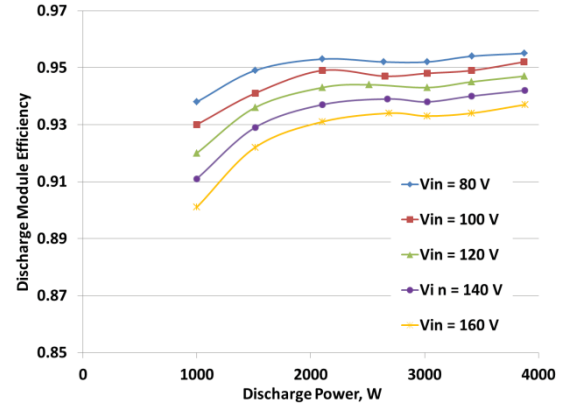


Figure 19. Discharge module efficiency for an output voltage of 400 V.

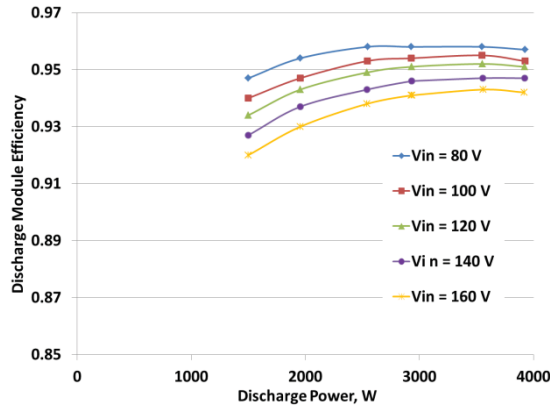


Figure 20. Discharge module efficiency for an output voltage of 500 V.

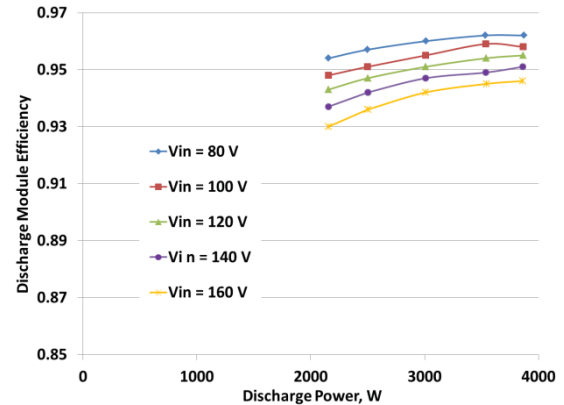


Figure 21. Discharge module efficiency for an output voltage of 600 V.

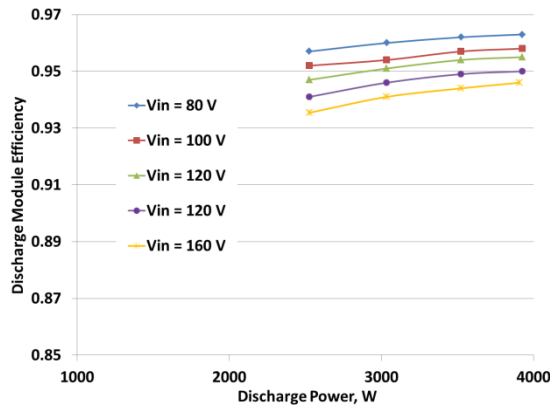


Figure 22. Discharge module efficiency for an output voltage of 650 V.

D. VACCO Xenon Flow Control Module Tests

D.1 Test Objectives

The main objective of testing the VACCO XFCM is to confirm that unit can operate in vacuum in stand-alone open and close loop modes. After successful completion of the stand-alone tests the unit was integrated tested with the HiVHAc EDU thruster (as is detailed in the next section).

D.2 VACCO XFCM Test Results

Standalone Tests of the VACCO XFCM unit were performed in VF5 and VF12. The VACCO XFCM test in VF5 represents the first time the unit has been tested in a vacuum chamber with a Hall thruster (results presented in Section 5A). As is shown in Figs. 7 and 23, the unit was not mounted on the thrust stand but was mounted on a bracket next to the thrust stand. This was done because the cable that controls and powers the XFCM required more terminals than was available on the thrust stand waterfall wiring harness. As shown in Fig. 6, MFC1 (200 sccm) fed the XFCM, the two outlets of the XFCM (going to the anode and cathode) were routed to the thrust stand. Solenoid valves were attached to the outlets of the XFCM to avail the option of using the laboratory feed system to supply xenon to the anode and cathode.

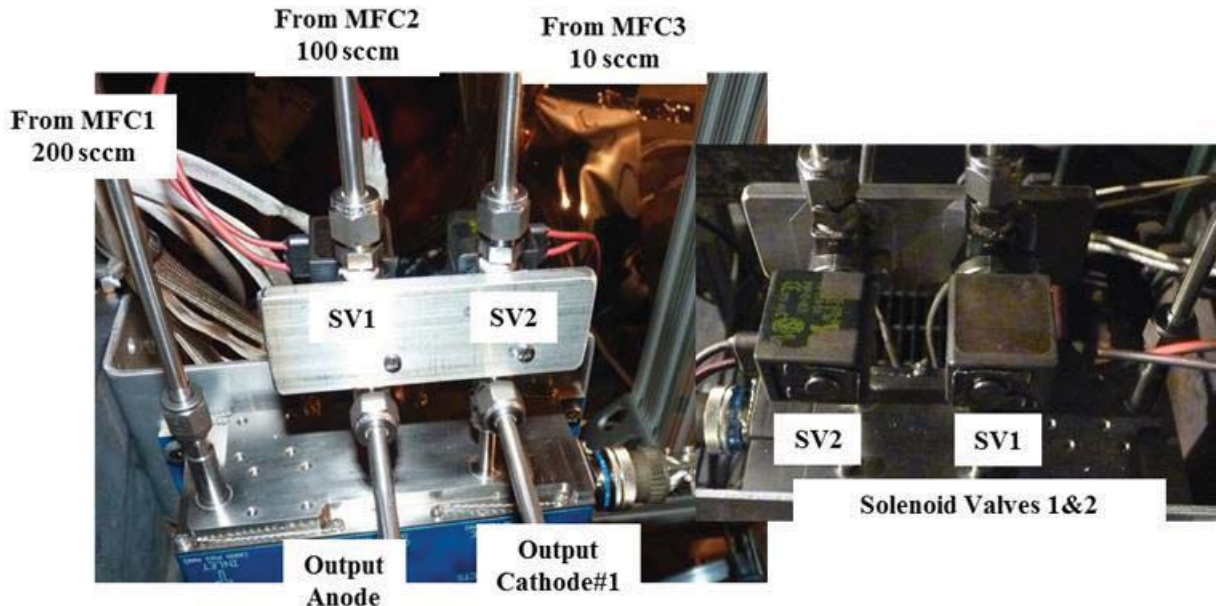


Figure 23. VACCO XFCM setup scheme inside VF5 allows for use of XFCM or laboratory MFCs to supply propellant to the HiVHAc EDU thruster that is mounted on the inverted pendulum thrust stand.

Figure 24 shows a schematic of the XFCM. For the VF5 test, the XFCM was operated in open loop. In open loop the voltage of PCV1 and PCV2 was adjusted until the desired flow rate through the XFCM was attained. Mass flow controller 1 was operated as a flow monitor. Standalone tests with the XFCM were performed at anode flow rates of approximately 1.8, 3.9, 4.9 and 6 mg/s. Test results that XFCM was capable of supplying and maintaining the desired and prescribed flows.

Additional tests with the XFCM were also performed in VF12. The XFCM setup for VF12 was modified from its earlier setup for VF5. The VF12 setup is shown in Fig. 25. The modifications included the addition of 3 solenoid valves. The original VF5 setup was modified to allow usage of the MFC supplying the XFCM to also supply the anode directly without having to go through the XFCM. In addition, the new setup allows the user to totally isolate the XFCM when not in use. The XFCM VF12 tests entailed operating the XFCM in closed loop of the pressure transducer reading

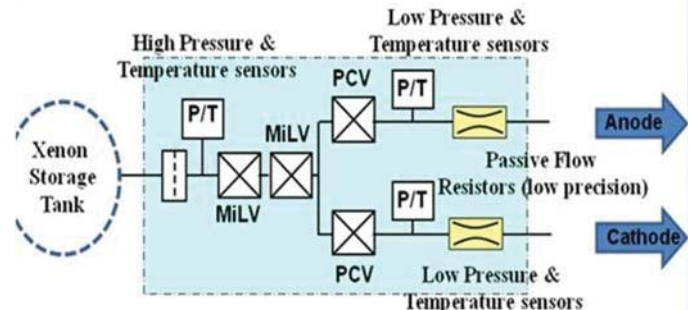


Figure 24. VACCO XFCM schematic.

downstream of the piezo proportional control valve (Fig. 24). Tests of the anode and cathode channels were performed in closed loop control and confirmed that we can accurately control and maintain the xenon flow to the thruster's anode and cathode. Testing was not performed with the thruster due to facility issues that prohibited thruster operation. When VF12 is back on-line closed loop tests of the HiVHAc EDU thruster with the VACCO XFCM will be performed. In addition, VACCO and NASA Glenn will modify the control software and the XFCM control box to permit operation of the VACCO XFCM in closed loop of the thruster discharge current telemetry signal.

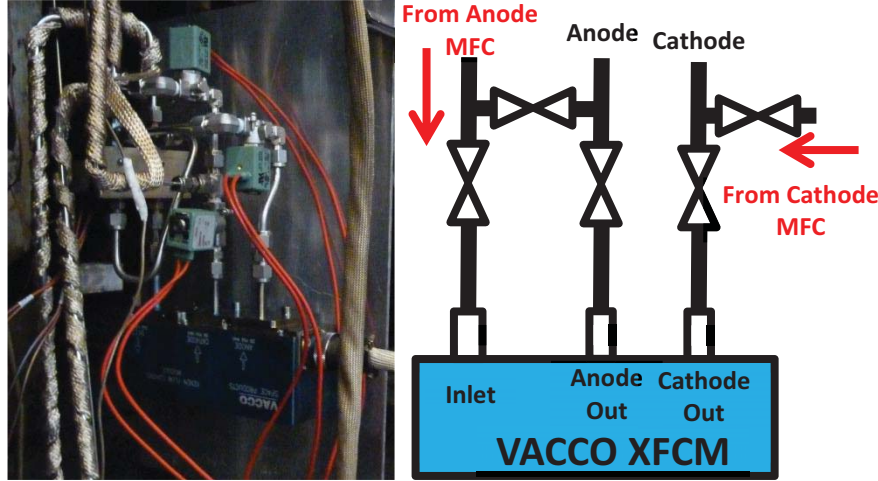


Figure 25. VACCO XFCM setup in VF12.

V. Integration Test of the HiVHAc System Components

A. Integration Test Objectives and Results

The main objective of the integrated test of the HiVHAc EDU thruster, BB1, and VACCO XFCM is to demonstrate thruster operation with the XFCM and to confirm that thruster performance is identical to test results when a laboratory xenon feed system is used. Previous tests confirmed that thruster performance with the BB1 PPU was identical to when laboratory power supplies were used. For this integrated test, the XFCM was operated in open loop as detailed earlier. Thruster and BB1 tests with the XFCM were performed at a discharge voltage of 650 V for anode flow rates of approximately 1.8, 3.9, 4.9 and 6 mg/s. Tests with the laboratory XFS were repeated at the same flow rates to confirm that the thruster operated in an identical fashion. For testing with the laboratory XFS, MFCs 2 and 3 were used (shown in Fig. 7). Table 3 summarizes the test results with the XFCM and the laboratory xenon feed system at a discharge voltage of 650 V. As is shown in Table 3, the thruster operation was invariant to which xenon feed system delivered the xenon to the thruster. The ratio of the thruster discharge currents and thrust was almost one at the different flow rates. In addition, the test confirmed that the XFCM is able to accurately supply and maintain the xenon supply rate to thruster.

Table 3. Comparison of thruster operation between the laboratory mass flow controllers and VACCO XFCM.

Laboratory MFC		VACCO XFCM		Ratio of VACCO XFCM to Laboratory MFC values		
Anode Flow Rate, mg/s	Discharge Current, A	Anode Flow Rate, mg/s	Discharge Current, A	Anode Flow Rate	Discharge Current	Thrust
1.99	1.82	2.00	1.8	1	1.01	1.01
3.91	3.70	3.91	3.67	1	1.01	1.01
4.91	4.74	4.91	4.79	1	0.99	1.00
6.02	5.97	6.00	6.04	1	0.99	1.00

B. HiVHAc System Components Validation Summary

Table 4 below summarizes the status of the HiVHAc system components validation. Table 2 shows that the xenon feed system is at TRL 6 and that the BB2 will be at TRL 5 once the thermal vacuum tests are completed in Q1 of FY14. The EDU thruster is planned to undergo a short duration (500-1,000 hrs) test in Q1 of FY14 to validate and demonstrate the in-situ self-regulating operation of the discharge channel replacement mechanism. This test will be followed by a thermal vacuum test at NASA Glenn in Q2/Q3 of FY14. A single-string integration test of the HiVHAc system will be performed after the delivery of another enhanced CPE PPU that will incorporate a circuit board that controls the VACCO XFCM.

Table 4. HiVHAc system component validation summary.

	HiVHAc EDU Thruster	Enhanced BB PPU	VACCO XFCM
Functional, Performance, and Vacuum Tests	Complete (VF12 and VF5)	Complete, 1,500 hrs in vacuum operation	Complete
Qual-Level Vibration Test	Complete	Complete*	Complete
Qual-Level Thermal Test	Planned FY14	Planned FY14/Q1	Complete

*Test performed by CPE but will be repeated at NASA Glenn.

VI. Summary and Future Plans

NASA's Science Mission Directorate In Space Technology Propulsion office is sponsoring the development of the 4 kW-class HiVHAc Hall propulsion system for implementation in NASA missions. The major components of the HiVHAc propulsion system include the HiVHAc EDU thruster, the CPE BB2 PPU, and the VACCO XFCM unit.

Recent mission analysis studies performed using the HiVHAc EDU throttle tables indicate that the HiVHAc thruster can close the four Discovery-class and the two New Frontiers-class DRMs. The same mission studies found that the Aerojet-Rocketdyne BPT-4000 was unable to close the New Frontiers-class DRMs.

The performance of the HiVHAc thruster was evaluated at NASA Glenn VF5. Tests in VF5 were performed at facility background pressure conditions that were 6-7 times lower than previously completed. Vacuum facility 5 HiVHAc thruster performance indicated reduced performance levels when compared to VF12 levels. This led the team to perform facility background sensitivity studies that are reported in a companion paper. Voltage-Current characterization of the HiVHAc thruster were performed at discharge voltages between 200 and 600 V, and for electromagnet settings that range between a nominal value of I_0 and $2 \cdot I_0$. HiVHAc's V-I profiles indicate that the thruster has a wide range of stable operation at electromagnet settings that are within the thruster's design limits.

Vacuum tests were performed on an enhanced CPE BB PPU. Peak discharge module efficiency of 96.3% was measured. To date, the unit's vacuum burn-in test has accumulated over 1,500 hours of full power (3.9 kW) operation. Standalone vacuum tests of the VACCO XFCM indicated that the unit was able to supply and maintain the required xenon flow rate in both open and closed loop modes.

Finally, an integrated components test of the HiVHAC EDU, BB1 PPU, and XFCM was performed. The test confirmed that the major components of the HiVHAc system resulted in nominal thruster operation and performance.

Future plans include:

- Perform a short duration test of the HiVHAc EDU thruster to confirm the operation of the in-situ self-regulating discharge channel replacement mechanism;
- Perform a thermal vacuum test of the HiVHAc EDU thruster;
- Evaluate performance of the HiVHAC EDU thruster in VF5 after the completion of the facility's pumping speed improvements that will allow us to test the thruster at background pressure magnitudes that are anticipated to be 2-3 times lower than what was reported in this paper;
- Perform a thermal vacuum and random vibration tests of the BB2 PPU;
- Test, in FY14/Q3; another high-fidelity flight-like PPU, designated as EM1 (engineering model 1), that will be delivered by CPE. This unit will incorporate some flight components and will also contain a

- circuit board that controls the VACCO XFCM; and
- Perform a single-string integration test of the HiVHAc EDU, EM1, and VACCO XFCM to quantify the performance of the HiVHAC propulsion system.

Acknowledgments

The authors would like to thank and acknowledge the Science Mission Directorate for funding this work. The authors also acknowledge the contributions of Aerojet-Rocketdyne, Colorado Power Electronics, and VACCO in helping develop and manufacture the HiVHAc system components. Lastly, the authors thank Kevin Blake, George Jacynycz, Michael McVetta, and James Mullins for helping assemble and install the thruster in the vacuum facility, as well as maintaining and operating the vacuum facility.

References

- ¹ Sovey, J. S., Rawlin, V. K., and Patterson, M. J., "Ion Propulsion Development Projects in U.S.: Space Electric Rocket Test to Deep Space 1," *Journal of Propulsion and Power*, Vol. 17, No. 3, May-June 2001, pp. 517-526.
- ² Russel, C. T., *et al.*, "Dawn: A Journey to the Beginning of the Solar System," DLR International Conference on Asteroids, Comets, and Meteors, July-August 2002.
- ³ Garner, C.E., Rayman, M.D., and Brophy, J.R., "In-Flight Operation of the Dawn Ion Propulsion System Through Year One of the Cruise to Ceres," AIAA-2013-4112, July 2013.
- ⁴ NASA's Science Mission Directorate Science Plan for 2007-2016.
- ⁵ Dankanich, J. W., "Electric Propulsion for Small Body Missions", AIAA Paper 2010-6614, August 2010.
- ⁶ Anderson, D. J., Munk, M., Pencil, E., Dankanich, J., Glaab, L., and Peterson, T., "The Status of Spacecraft Bus and Platform Technology Development under the NASA ISPT Program," IEEEAC Paper No. 2138, 2013 IEEE Aerospace Conference, Big Sky, MT, March 2-9, 2013
- ⁷ Shastry, R., Herman, D. A., Soulard, G. C. and Patterson, M. J., "Status of NASA's Evolutionary Xenon Thruster (NEXT) Long-Duration Test as of 50,000 h and 900 kg Throughput," 33rd International Electric Propulsion Conference, IEPC-2013-121, Washington D.C., 6-10 Oct, 2013.
- ⁸ Dankanich, J.W., Drexler, J. A., and Oleson, S. R., "Electric Propulsion Mission Viability with the Discovery-Class Cost Cap," AIAA Paper 2010-6776, August 2010.
- ⁹ Oh, D. "Evaluation of Solar Electric Propulsion Technologies for Discovery Class Missions," AIAA Paper 2005-4270, July 2005.
- ¹⁰ Witzberger, K. E., *et al.*, "NASA's 2004 In-Space Propulsion Re-focus Studies for New Frontiers Class Missions," AIAA Paper 2005-4271, July 2005.
- ¹¹ Jacobson, D., *et al.* "NASA's 2004 Hall Thruster Program," AIAA Paper 2004-3600, July 2004.
- ¹² Manzella, D., Oh, D., and Aadland, R., "Hall Thruster Technology for NASA Science Missions," AIAA Paper 2005-3675, Tucson, Arizona, 2005.
- ¹³ Dankanich, J., Kamhawi, H., and Mathers, A., "HiVHAc Maximum Operating Power Range," IEPC Paper 2009-213, September 2009.
- ¹⁴ Kamhawi, H., *et al.*, "Performance and Environmental Test Results of the High Voltage Hall Accelerator Engineering Development Unit," AIAA 2012-3854, July 2012.
- ¹⁵ Hofer, R.R., "High-Specific Impulse Operation of the BPT-4000 Hall Thruster for NASA Science Missions,", AIAA 2010-6623, July 2010.
- ¹⁶ Hesterman, B., "Wide Range Multi-Phase Resonant Converters," JANNAF-1435, May 2010.
- ¹⁷ Pinero, L. R., Kamhawi, H., and Drummond, G., "Integration Testing of a Modular Discharge Supply for NASA's High Voltage Hall Accelerator Thruster," IEPC Paper 2009-275, September 2009.
- ¹⁸ Kamhawi, H., Huang, W., Haag, T., and Spektor, R., "Investigation of the Effects of Facility Background Pressure on the Performance and Voltage-Current Characteristics of the High Voltage Hall Accelerator," 33rd International Electric Propulsion Conference, IEPC-2013-446, Washington, DC, 6-10 Oct, 2013.
- ¹⁹ Pinero, L. R., Kamhawi, H., and Drummond, G., "Integration Testing of a Modular Discharge Supply for NASA's High Voltage Hall Accelerator Thruster", 31st International Electric Propulsion Conference, 2009-275, Ann Arbor, MI, 20-24 Sep., 2009.
- ²⁰ Huang, W., Kamhawi, H., and Haag, T., "Effect of Background Pressure on the Performance and Plume of the

HiVHAc Hall Thruster”, 33rd International Electric Propulsion Conference, IEPC-2013-058, Washington, DC, 6-10 Oct, 2013.

²¹ Kamhawi, H., Huang, W., Haag, T., and Spektor, R., “Investigation of the Effects of Facility Background Pressure on the Performance and Voltage-Current Characteristics of the High Voltage Hall Accelerator,” 33rd International Electric Propulsion Conference, IEPC-2013-446, Washington, DC, 6-10 Oct, 2013.